

Chalcogenapyrylium Dyes as Potential Photochemotherapeutic Agents. Solution Studies of Heavy Atom Effects on Triplet Yields, Quantum Efficiencies of Singlet Oxygen Generation, Rates of Reaction with Singlet Oxygen, and Emission Quantum Yields

Michael R. Detty* and Paul B. Merkel*

Contribution from the Corporate Research Laboratories and Photographic Research Laboratories, Eastman Kodak Company, Rochester, New York 14650. Received September 18, 1989

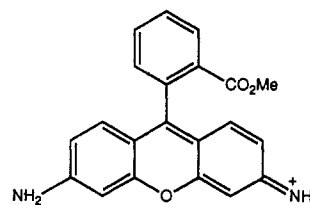
Abstract: Chalcogenapyrylium dyes of general structure **1** were examined in methanolic solution with respect to the generation of singlet oxygen. Heavy atom effects are pronounced with quantum yields of singlet oxygen generation [$\Phi(^1O_2)$] increasing from 0.0004 for pyrylium dye (**1a**) to 0.12 for tellurapyrylium dye (**1j**). Oxygen concentration studies gave triplet yields (Φ_T) of 0.18 for **1j** and 0.11 for **1i** and estimated triplet lifetimes (τ_T) of 0.3 and 0.8 μ s, respectively, in methanol. Similar lifetimes were determined in water. Selenapyrylium dye (**1f**) was found to have τ_T of $\geq 10 \mu$ s such that Φ_T and $\Phi(^1O_2)$ should be equivalent. Variations in rate constants for intersystem crossing were found to be the dominant factor in controlling triplet yields. Values of $\Phi(^1O_2)$ were found to be sensitive to methyl substitution in the hydrocarbon backbone. Increased steric interactions were found to lower values of $\Phi(^1O_2)$ in methyl-substituted dyes **2** and **4** relative to unsubstituted dyes **1** and **3**. The same methyl-substituted compounds showed lower quantum yields for fluorescence, suggesting increased rates of radiationless decay in both S_1 and T_1 states. Tellurapyrylium dyes were much more reactive with singlet oxygen than the other chalcogenapyrylium dyes, giving products **5** derived from formal oxidative addition of hydrogen peroxide across tellurium. Singlet oxygen was determined to be the oxidant under photooxidation conditions of tellurapyrylium dyes based on the similarity of reactivities measured with rose bengal and methylene blue as singlet oxygen sensitizers, on increased rates of reaction in deuterated solvents, on much slower rates of reaction of hydrogen peroxide with tellurapyrylium dyes, and on the formation of different products upon the reaction of superoxide with tellurapyrylium dyes.

Photochemotherapy or photodynamic therapy (PDT) is a relatively recent development in cancer therapy that employs light as an integral part of the treatment. Light can be delivered selectively to the area of treatment through the use of catheters and fiber optic cables. Unlike laser surgery that employs light energy to generate a thermal scalpel, PDT employs a drug called a photosensitizer, which is activated by light to undergo a chemical reaction that produces a cytotoxic agent. Ideally, the photosensitizer is localized in or around the tumor mass, is nontoxic to normal tissues, is activated by light that can penetrate deeply into both tumor and tumor-involved normal tissues, and is photochemically efficient in producing the cytotoxic agent.¹ Such an agent would allow the selective destruction of neoplastic tissue while leaving normal tissue intact.

A variety of photosensitizers have been examined for use in PDT including fluorescein, eosin, tetracycline, acridine orange, hematoporphyrin derivative (HpD) and related porphyrins, phthalocyanines, and metallophthalocyanines.²⁻⁸ For most applications of PDT, the cytotoxic agent is produced by one of two different processes called type I and type II. In a type I process, the absorption of a photon by the photosensitizer leads to radical

species (via electron transfer) that function as the cytotoxic agents. In type II processes, oxygen reacts with an excited state of the photosensitizer to produce either superoxide radical anion (via electron transfer) or singlet oxygen (via triplet-triplet interactions). Only recently have chemists applied their knowledge of physical and photophysical properties to the design of sensitizers for PDT.^{1c,e,f,8}

Studies with rhodamine 123 (Rh-123) have been of particular interest in the design of a photosensitizer. Rh-123 is a cationic dye that is specifically taken up by the mitochondria of living cells.⁹ It has been suggested that the electrochemical gradient driven by respiratory electron transport in the mitochondria and the pH gradient generated by the mitochondrial proton pump are responsible for the selective mitochondrial uptake of Rh-123.^{10,11}



Rhodamine 123

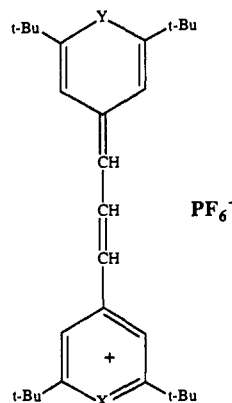
It has been demonstrated that Rh-123 accumulates more in carcinoma cells and muscle cells relative to other body cell types¹¹ and that Rh-123 is selectively toxic to carcinoma cells in vitro.¹²⁻¹⁴ Presumably, the greater metabolic activity of cancer cells (and

- (1) (a) Dougherty, T. J. *Photochem. Photobiol.* **1987**, *45*, 879. (b) Powers, S. K.; Pribil, S.; Gillespie, G. Y.; Watkins, P. J. *J. Neurosurg.* **1986**, *64*, 918. (c) Ben-Hur, E.; Rosenthal, I. *Photochem. Photobiol.* **1985**, *42*, 129. (d) Ben-Hur, E.; Carmichael, A.; Riesz, P.; Rosenthal, I. *Int. J. Radiat. Biol.* **1985**, *48*, 837. (e) Morgan, A. R.; Garbo, G. M.; Kreimer-Birnbaum, R.; Keck, R. W.; Chaudhuri, K.; Selman, S. H. *Cancer Res.* **1987**, *47*, 496. (f) Oseroff, A. R.; Ohuoha, D.; Ara, G.; McAuliffe, D.; Foley, J.; Cincotta, L. *Proc. Natl. Acad. Sci. U.S.A.* **1986**, *83*, 9729.
- (2) Figge, F. H. J.; Weiland, G. S.; Manganiello, L. O. *J. Proc. Soc. Exp. Biol. Med.* **1948**, *68*, 640.
- (3) Kochevar, I. E.; *J. Invest. Dermatol.* **1981**, *77*, 59.
- (4) Moore, G. E. *Science (Washington, D.C.)* **1947**, *106*, 130.
- (5) Rall, D. P.; Loo, T. L.; Lane, M. *JNCI* **1957**, *19*, 79.
- (6) Rassmussen-Taxdal, D. S.; Ward, G. E.; Figge, F. H. *J. Cancer* **1955**, *8*, 78.
- (7) (a) Dougherty, T. J.; Thoma, R. E.; Boyle, D. G.; Weishaupt, K. R. *Cancer Res.* **1981**, *41*, 401. (b) Weishaupt, K. R.; Gomer, C. J.; Dougherty, T. J. *Cancer Res.* **1976**, *36*, 2326. (c) Stenstrom, A. G. K.; Moan, J.; Brunborg, G.; Eklund, T. *Photochem. Photobiol.* **1980**, *32*, 349.
- (8) Firey, P. A.; Ford, W. E.; Sounik, J. R.; Kenney, M. E.; Rogers, M. A. G. *J. Am. Chem. Soc.* **1988**, *110*, 7626.

- (9) Johnson, L. V.; Walsh, M. L.; Chen, L. B. *Proc. Natl. Acad. Sci. U.S.A.* **1980**, *77*, 990.
- (10) Mitchell, P. *Chemiosmotic Coupling in Oxidative and Photosynthetic Phosphorylation*, Glynn Research Ltd.: Bodmin, England, 1966; pp 1-205.
- (11) Summerhayes, I. C.; Lampidis, T. J.; Bernal, S. D.; Chen, L. B. *Proc. Natl. Acad. Sci. U.S.A.* **1982**, *79*, 5292.
- (12) Lampidis, T. J.; Bernal, S. D.; Summerhayes, I. C.; Chen, L. B. *Ann. N.Y. Acad. Sci.* **1982**, *395*, 299.
- (13) Lampidis, T. J.; Bernal, S. D.; Summerhayes, I. C.; Chen, L. B. *Cancer Res.* **1983**, *43*, 716.
- (14) Bernal, S. D.; Lampidis, T. J.; Summerhayes, I. C.; Chen, L. B. *Science (Washington, D.C.)* **1982**, *218*, 1117.

muscle cells) relative to normal cells leads to an increased membrane potential in tumor cells relative to normal cells.¹⁵ Although Rh-123 has been examined as a photosensitizer for PDT,^{16,17} Rh-123 absorbs light of too short a wavelength for good tissue penetration and produces singlet oxygen only inefficiently upon irradiation.

Structurally, the rhodamine dyes are benzo-fused members of the pyrylium class of dyes. We have been interested in the heavier chalcogens sulfur, selenium, and tellurium incorporated into pyrylium rings and the resulting effects on spectral, physical, photophysical, and biological properties. In a preliminary communication,¹⁸ we described the efficient production of singlet oxygen upon irradiation of air-saturated methanolic solutions of tellurapyrylium dyes and the rapid reaction of tellurapyrylium dyes with singlet oxygen in the presence of water. Tellurapyrylium dyes have also been found to be useful in vitro against different malignant glioma cell lines¹⁹ and have been found to be taken up by tumor tissue, presumably via mitochondrial localization.^{19b} Herein, we extend the scope of our earlier work¹⁸ to include a more thorough exploration of the physical and photophysical properties of the chalcogenapyrylium dyes **1** and substituted analogues with



- 1a**; X = Y = O (ClO₄⁻) **1f**; X = Y = Se
1b; X = S, Y = O (ClO₄⁻) **1g**; X = Te, Y = O
1c; X = Y = S **1h**; X = Te, Y = S
1d; X = Se, Y = O **1i**; X = Te, Y = Se
1e; X = Se, Y = S **1j**; X = Y = Te

respect to their abilities to generate singlet oxygen and to react with singlet oxygen. In particular, quantitative assessments of heavy atom effects with respect to lifetimes, triplet yields, and rates of intersystem crossing are made. Such studies should aid in the design of other cationic sensitizers for photodynamic therapy.

Results and Discussion

Parameters of Photosensitizer Design. In designing chalcogenapyrylium dyes for use as photosensitizers for PDT, a set of dye requirements should be met. The dye should absorb wavelengths of light that offer maximum transmission of light through tissue. At wavelengths of light below 600 nm, the depth of nonthermal penetration of light is limited to a few millimeters due to competitive absorption of light by biological molecules.²⁰

(15) Pederson, P. L. *Prog. Exp. Tumor Res.* **1978**, *22*, 190.

(16) Powers, S. K.; Pribil, S.; Gillespie, G. Y.; Watkins, P. J. *J. Neurosurg.* **1986**, *64*, 918.

(17) Beckman, W. C., Jr.; Powers, S. K.; Brown, J. T.; Gillespie, G. Y.; Bigner, D. D.; Camps, J. L., Jr. *Cancer* **1987**, *59*, 266.

(18) Detty, M. R.; Merkel, P. B.; Powers, S. K. *J. Am. Chem. Soc.* **1988**, *110*, 5920.

(19) (a) Powers, S. K.; Walstad, D. L.; Brown, J. T.; Detty, M. R.; Watkins, P. J. *J. Neuro-Oncol.* **1989**, *7*, 179. (b) Detty, M. R.; Merkel, P. B.; Hilf, R.; Gibson, S. L.; Powers, S. K. *J. Med. Chem.* Submitted for publication.

(20) Wan, S.; Parrish, J. A.; Anderson, R. R.; Madden, M. *Photochem. Photobiol.* **1981**, *34*, 679.

Table I. Spectral and Redox Properties for Chalcogenapyrylium Dyes **1** and **2**

compd	$\lambda_{\max}(\text{H}_2\text{O}),$ nm	log ϵ	E_{pa}^a , V	E_{red}^a , V
1a	593	5.31	+0.92	-0.75
1b	640	5.32	+0.84	-0.68
1c	685	5.42	+0.72	-0.62
1d	665	5.38	+0.71	-0.61
1e	708	5.40	+0.82	-0.54
1f	730	5.48	+0.75	-0.50
1g	700	5.27	+0.78	-0.56
1h	755	5.02	+0.73	-0.50
1i	770	5.10	+0.94 ^b	-0.42 ^b
1j	810	5.22	+0.86 ^b	-0.32 ^b
2a	843 ^b	5.42	+0.82 ^b	-0.35 ^b
2b	801 ^b	5.44	+0.87 ^b	-0.40 ^b
2c	803 ^b	5.44	+0.87 ^b	-0.40 ^b
2d	760	5.38	+0.69	-0.52
2e	782	4.86	+0.65	-0.51

^a Approximately 5×10^{-4} M in acetonitrile with 0.1 M tetrabutylammonium tetrafluoroborate as supporting electrolyte at a Pt disk electrode vs SCE at a scan rate of 0.1 V s⁻¹. ^b In dichloromethane as solvent.

However, above 600 nm, up to the absorption of the harmonics of the infrared absorption of water stretching at approximately 1250 nm, biological tissue is much more transparent to light.²⁰ HpD and other porphyrins, as well as the rhodamines, absorb weakly at wavelengths above 600 nm, which limits their utility as photosensitizers for PDT.

The chalcogenapyrylium dye as photosensitizer should be relatively stable in the biological environment and should have a relatively long half-life in the dark in serum and in the tissues undergoing PDT. The susceptibility of the dye to reduction in vivo can be predicted by the redox potentials of the dye in solution. Aqueous solubility of the compound should be sufficient to allow intravascular injection of the photosensitizer. Neither the dye nor its metabolites should be toxic to normal tissues at the doses required for PDT.

The photosensitizer, following production of a lethal amount of the cytotoxic agent, should ideally be bleached during PDT or be converted temporarily to a form that no longer absorbs the activating wavelength of light. This is necessary in order that the dye will not act as a chromophore in the treated tissue and screen the light from reaching tumor cells deeper in tissue for photoactivation. This phenomenon of the photosensitizer limiting the depth of tissue treated by PDT has been described with HpD and is called the "shielding effect".²¹

Chalcogenapyrylium Dyes Chosen as Photosensitizers for PDT.

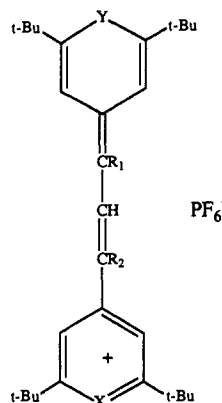
The chalcogenapyrylium dyes that have exhibited significant potential for PDT are of general structure **1** where X and Y are some combination of oxygen, sulfur, selenium, or tellurium atoms. The *tert*-butyl substituents impart greater kinetic stability toward the biological environment. The trimethine bridge connecting the two heterocyclic rings extends the absorption maximum for many of the dyes to the near infrared, well beyond where biological tissues absorb. The effects of changing X and Y and of introducing substituents on the trimethine bridge connecting the two rings can be examined with respect to wavelength of absorption, redox potentials, quantum efficiencies for fluorescence, quantum yields for both the production of triplets and the generation of singlet oxygen, and rates of reaction with singlet oxygen. The principles developed here should be applicable to the design of other cationic photosensitizers for PDT.

The wavelength of absorption of dyes of structure **1** varies by over 200 nm as a function of the chalcogen atoms X and Y. While dye **1a** with X = Y = O absorbs light with a maximum of absorption at 590 nm in water (Table I), dye **1j** with X = Y = Te absorbs light with a maximum of absorption at 810 nm in water (Table I). These shifts are consistent with the wavelength changes

(21) Dorion, D. R.; Svaasand, L. O.; Profio, A. E. *Adv. Exp. Med. Biol.* **1981**, *160*, 63.

observed for other chalcogenapyrylium dyes of similar structure.²² As the heteroatoms increase in molecular weight in dyes **1**, the oxidation potentials become more negative and the reduction potentials become more positive (Table I). In addition to predicting the ease of reduction and/or oxidation in vivo, the changes in oxidation and reduction potentials should reflect changes in the HOMO-LUMO gap.^{22b} Thus, in these compounds **1**, the HOMO-LUMO gap narrows and the S_0 - S_1 transition requires less energy as the chalcogen atoms become heavier. Consequently, a bathochromic shift is observed by narrowing the differences in energy between these levels.

Trimethine dyes **2** show the effect of substitution on the trimethine bridge in dyes **1** with respect to wavelength of absorption and redox potentials as compiled in Table I. In the trimethine dyes **2**, each methyl substituent imparts approximately a 15-nm



2a; X = Y = Te, R₁ = H, R₂ = Me

2b; X = Te, Y = Se, R₁ = H, R₂ = Me

2c; X = Te, Y = Se, R₁ = Me, R₂ = H

2d; X = Y = Se, R₁ = H, R₂ = Me

2e; X = Y = Se, R₁ = R₂ = Me

bathochromic shift. The redox potentials for the dyes **2** show that nearly all of the narrowing of the S_0 - S_1 gap comes from raising the energy of the HOMO level (as reflected in the oxidation potentials).

Fundamentals of the Photophysics Associated with Cationic Dyes. An understanding of the photophysics associated with the cytotoxicity of cationic dyes facilitates the design of improved photosensitizers for PDT. Cationic dyes, such as the rhodamines and the chalcogenapyrylium dyes, could function as a photosensitizer by either a type I or a type II process. Both the formation of radicals (from a type I process) and the formation of superoxide radical anion (from a type II process) are the result of single-electron transfer (SET) involving an excited state of the dye. Typically, cationic dyes are characterized by reversible one-electron oxidations and reductions in the ground (S_0) state.^{22b} In the first excited (S_1) state, following promotion of an electron, both oxidation and reduction of the dye will be energetically more favorable by approximately the energy of the absorbed photon. The excited dye is, thus, both a more powerful reducing agent and a more powerful oxidizing agent than the ground state of the dye. SET between the excited state of the dye and surrounding biological molecules can produce radicals while SET from the excited state of the dye to ground-state ($^3\Sigma_g^-$) oxygen (3O_2) produces superoxide radical anion. The S_1 states of cationic dyes, such as **1**, are short-lived species with lifetimes of less than 10 ns. Internal conversion, cis-trans isomerization, and fluorescence can quickly return the S_1 state to the S_0 state. If intersystem crossing occurs from the S_1 state to the first triplet (T_1) state, much longer lived species are produced. The T_1 state of the dye can react with ground-state oxygen via a spin-allowed process to produce the S_0

Table II. Quantum Efficiencies [$\Phi(^1O_2)$] for Generation of and Rates of Reaction [$k(^1O_2)$] with Singlet Oxygen for Chalcogenapyrylium Dyes

compd	$\Phi(^1O_2)^a$	$10^2k(^1O_2)$, M ⁻¹ s ⁻¹	
		methylene blue ^b	rose bengal ^b
1a	0.0004 ± 0.0001		0.3 ± 0.1
1c	0.0006 ± 0.0001		1.3 ± 0.1
1d	0.004 ± 0.001	0.3 ± 0.1	0.4 ± 0.1
1e	0.007 ± 0.001		
1f	0.013 ± 0.002		0.5 ± 0.1
1g	0.05 ± 0.01	8.5 ± 0.9	9.4 ± 0.9
1h	0.07 ± 0.01		
1i	0.09 ± 0.01		
1j	0.12 ± 0.01	17.6 ± 1.0	17.8 ± 1.0
2d	0.004 ± 0.001		
2e	0.001 ± 0.0003		
3	0.07 ± 0.01		
4	0.006 ± 0.002		

^a In methanol. ^b In 50% aqueous methanol.

state of the dye and the first excited state ($^1\Delta_g$) of oxygen, singlet oxygen (1O_2), which is the other component of type II reactions.

Singlet oxygen lies approximately 23 kcal/mol higher in energy than ground-state oxygen. The energy of the T_1 state of the dye should lie close to or higher than this energy relative to the energy of the S_0 state for efficient production of singlet oxygen.⁸ In porphyrin and phthalocyanine systems where molecular orbitals are benzene-like, the S_1 - T_1 splittings are quite large, on the order of approximately 15 kcal/mol. To produce singlet oxygen in systems of this type, the energy of the absorbed photon must be at least 38 kcal/mol, which corresponds to a wavelength of 750 nm or shorter. Cationic dyes have S_1 - T_1 splittings that are much smaller, typically 8–12 kcal/mol (3000–4000 cm⁻¹).²³ Thus, the energy of the absorbed photon need only be on the order of 31–35 kcal/mol, which corresponds to a wavelength of approximately 900 nm or shorter. Near-infrared-absorbing chalcogenapyrylium dyes of structure **1** should have a T_1 state with sufficient energy to produce singlet oxygen.

Solution Studies of Singlet Oxygen Generation with Chalcogenapyrylium Dyes. In using chalcogenapyrylium dyes as photosensitizers, the ability of each dye to either undergo SET or produce triplet states for the production of singlet oxygen should be considered. In this class of compounds, the heteroatom effects show opposite trends with respect to SET and triplet yield. Because the S_0 and S_1 splitting narrows as the heteroatoms become heavier, the excited-state pyrylium dyes are going to be the most powerful oxidizing agents and reducing agents while excited-state tellurapyrylium dyes are going to be the least powerful. Intersystem crossing from the S_1 state to the T_1 state can be promoted by increased spin-orbit coupling between an attached heavy atom and the molecular orbitals of the dye.^{23,24} As the heteroatoms become heavier, spin-orbit coupling should increase such that tellurapyrylium dyes should produce higher triplet yields than pyrylium dyes.

The quantum efficiency for the production of singlet oxygen [$\Phi(^1O_2)$] will be, to some extent, proportional to the triplet yield of the excited dye. This suggests that pyrylium dyes should be the least efficient at producing singlet oxygen while tellurapyrylium dyes should be the most efficient at producing singlet oxygen in dyes of structure **1**. Quantum yields for singlet oxygen generation in air-saturated methanol were determined by monitoring the chalcogenapyrylium dye-sensitized photooxidation of 1,3-diphenylisobenzofuran (DPBF). DPBF is a convenient acceptor since it absorbs in a region of chalcogenapyrylium dye transparency and rapidly scavenges singlet oxygen to form colorless products. Values of $\Phi(^1O_2)$ for the dyes **1** are compiled in Table II and show that the quantum yield increases from 0.0004 for pyrylium dye **1a** to 0.12 for tellurapyrylium dye **1j**. This trend

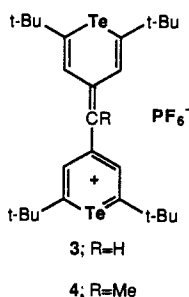
(23) McGlynn, S. P.; Azumi, T.; Kinoshita, M. In *Molecular Spectroscopy of the Triplet State*; Prentice Hall: Englewood Cliffs, NJ, 1969; pp 172–174.

(24) Turro, N. J. In *Modern Molecular Photochemistry*; Benjamin Cummings: Menlo Park, CA, 1978.

(22) (a) Detty, M. R.; Murray, B. J. J. *Org. Chem.* **1982**, *47*, 5235. (b) Detty, M. R.; McKelvey, J. M.; Luss, H. R. *Organometallics* **1988**, *7*, 1131.

is as expected on the basis of heavy atom effects on rate constants for intersystem crossing (k_{isc}).^{18,25}

Although heavy atom effects can increase values of $\Phi(^1O_2)$ through spin-orbit coupling effects, other substituent changes can lower quantum efficiencies for singlet oxygen production. X-ray structural analyses of chalcogenapyrylium dyes have shown them to be reasonably flat molecules.^{22b,26} The introduction of substituents that can disrupt the planarity of the molecule might promote nonradiative, internal conversion back to ground state, which could lower triplet yield, or might inhibit the interaction of the triplet state of the dye with ground-state oxygen, which could also lower the quantum efficiency of singlet oxygen generation. Values of $\Phi(^1O_2)$ for methyl-substituted chalcogenapyrylium dyes **2** and **4** can be compared with those for the unsubstituted dyes **1** and **3**. Methyl substitution in the methine



or trimethine bridge lowers the values of $\Phi(^1O_2)$ in both dye classes although the effect is much more pronounced in the monomethine dye **4** (Table II). This may reflect a more rapid radiationless decay of S_1 or T_1 states. The broader spectral bandwidths of **2** and **4** (≈ 100 nm) when compared with those of **1** and **3** (≈ 40 nm) suggest a less rigid structure in the methyl-substituted molecules.

Oxygen Concentration Effects. By measurement of photooxidation efficiencies as a function of oxygen concentration, it is possible to determine quantum yields for formation of dye triplets (Φ_T) and to estimate triplet lifetimes (τ_T). The oxygen concentration can be varied by bubbling the dye solutions with various partial pressures of oxygen. In methanol, the saturation oxygen concentration obtained by bubbling with pure oxygen at 1 atm was taken as 0.010 M.²⁷ For the chalcogenapyrylium dyes, lifetimes of the S_1 state are short (vide infra), such that oxygen quenching of this state and the generation of singlet oxygen thereby may be neglected. If the self-sensitized photooxidation of a chalcogenapyrylium dye ($\Phi_{ox,ss}$), at a fixed dye concentration and light intensity, is measured at various oxygen concentrations, then the photooxidation efficiency is given by

$$\Phi_{ox,ss} = \Phi(^1O_2)f = \Phi_T\{k_2[O_2]/(k_2[O_2] + k_1)\}f \quad (1)$$

where k_1 is the rate constant for phosphorescence and radiationless decay of the T_1 state to the S_0 state; k_2 is the rate constant for energy transfer from the T_1 state of the dye to the $^3\Sigma_-$ state of oxygen; and f , which remains constant, is the fraction of singlet oxygen scavenged by dye. Inverting eq 1 gives

$$1/\Phi_{ox,ss} = \{1/(\Phi_T f)\}\{1 + 1/(k_2\tau_T[O_2])\} \quad (2)$$

Thus, a plot of the inverse of the self-sensitized photooxidation yield or rate versus the inverse of $[O_2]$ should yield a straight line with an intercept/slope equal to the product of k_2 and τ_T . Since $\Phi(^1O_2)$ values have to be determined from the photosensitized fade of DPBF, triplet quantum yields can be calculated from

$$\Phi_T = \Phi(^1O_2)\{1 + 1/(k_2\tau_T[O_2])\} \quad (3)$$

Alternatively, measurement of efficiencies or rates (R) of self-sensitized photooxidation in air- and oxygen-saturated solutions allows calculation of $k_2\tau_T$ from

$$k_2\tau_T = \{1 - (R_{ox}[O_2]_{air}/R_{air}[O_2]_{ox})\}/\{[O_2]_{air}(R_{ox}/R_{air} - 1)\} \quad (4)$$

A $k_2\tau_T$ value of 900 ± 100 M⁻¹ and a Φ_T value of 0.18 were calculated in this manner for tellurapyrylium dye **1j** in methanol. If k_2 is assumed to have a value of about 3×10^9 M⁻¹ s⁻¹ (typical for oxygen quenching of triplets),^{23,28} then τ_T is estimated to be approximately 0.3 μ s.

By comparing the self-sensitized fade of **1j** in air-saturated and oxygen-saturated water (other conditions being constant), a value of $k_2\tau_T$ of 1000 ± 100 M⁻¹ was determined, which also suggests a triplet lifetime of 0.3 μ s. In these experiments, some dye fade occurs in the absence of irradiation, especially in oxygenated methanol. The photolytic bleaching was corrected for this thermal reaction.

In a similar manner, a $k_2\tau_T$ value of 2400 ± 1000 M⁻¹ was measured for dye **1i** in methanol. The large uncertainty in this value reflects a greater ratio of thermal to photolytic dye fading. Again, if k_2 is taken as 3×10^9 M⁻¹ s⁻¹, then τ_T for **1i** would be about 0.8 μ s. From the singlet oxygen yield of 0.09, a triplet yield of 0.11 is estimated for **1i** in methanol. Thus, nearly all of the dye triplets are quenched by oxygen in this case. Measurements in water, where the proportion of photolytic fade is increased, yield a $k_2\tau_T$ of 2700 ± 500 M⁻¹ and an estimated triplet lifetime of 0.9 μ s.

For selenapyrylium dye **1f**, self-sensitized photooxidation yields in air- and oxygen-saturated methanol were the same within experimental error (which is large in this case due to a relatively low photolytic fade rate). In water, where the ratio of photolytic to thermal bleaching is increased, it is possible to estimate that $k_2\tau_T$ is at least 30 000 M⁻¹, which implies a triplet lifetime of ≥ 10 μ s. For dye **1f**, the triplet yield is essentially the same as the singlet oxygen yield. (For dyes **1a-e**, the singlet oxygen yields may be assumed to be identical with the triplet yields since triplet lifetimes would be expected to be much longer in **1a-e** than in tellurapyrylium dyes **1g,h** where heavy atom effects are more pronounced.)

Rate Constants for Reaction of Chalcogenapyrylium Dyes with Singlet Oxygen. In chalcogenapyrylium dyes of structure **1**, singlet oxygen might attack the hydrocarbon backbone of the dye or the heteroatoms incorporated in the dye chromophore. Pyrylium dyes should only be attacked in the hydrocarbon framework. Both the heteroatoms and the hydrocarbon framework of sulfur-, selenium-, or tellurium-containing chalcogenapyrylium species could be oxidized by singlet oxygen.^{18,29} Rates of reaction [$k(^1O_2)$] of the dyes **1** with singlet oxygen in 50% aqueous methanol are compiled in Table II. These values were determined by the rate of reaction of the dye with singlet oxygen generated by irradiation of methylene blue and/or rose bengal in aqueous methanol solutions. Where comparative measurements were carried out, rate constants determined with rose bengal and methylene blue as sensitizers were similar.

Tellurapyrylium dye **1j** is most reactive with singlet oxygen, having a rate constant of 1.8×10^8 M⁻¹ s⁻¹ in 50% aqueous methanol. Substitution of an oxygen for one tellurium atom (**1g**) reduces reactivity by approximately 2-fold as might be expected statistically if the heteroatom were the primary site of reaction. The reactivities of selenapyrylium dyes **1f** and **1d** with singlet oxygen are more than an order of magnitude less than the reactivities of the tellurapyrylium dyes. Interestingly, thiapyrylium dye **1c** is much more reactive than the selenapyrylium dyes toward singlet oxygen.

The higher reactivity of the tellurium-containing dyes appears to reflect reaction at the tellurium atom. Upon sensitized photooxidation with singlet oxygen in water or aqueous methanol,

(25) Procedures for measuring $\Phi(^1O_2)$ values with 1,3-diphenylisobenzofuran and for obtaining $k(^1O_2)$ values are described in: Merkel, P. B.; Smith, W. F. *J. Phys. Chem.* **1979**, *83*, 2834.

(26) Detty, M. R.; Luss, H. R. *Organometallics* **1986**, *5*, 2250.

(27) Zinke, W. F.; Seidell, A. In *Solubilities of Inorganic and Metal-Organic Compounds*; American Chemical Society: Washington, DC, 1965; Vol. 11, p 1235.

(28) Values of k_2 have been measured independently by Prof. A. A. Gorman, Manchester, and have been found to be approximately 3×10^9 for dyes **1f**, **1i**, and **1j**. We thank Prof. Gorman for communicating his results to us prior to publication.

(29) (a) Liang, J.-J.; Gu, C.-L.; Kacher, M. L.; Foote, C. S. *J. Am. Chem. Soc.* **1983**, *105*, 4717 and references cited therein. (b) Kacher, M. L.; Foote, C. S. *Photochem. Photobiol.* **1979**, *26*, 765. (c) Akasaka, T.; Kako, M.; Sonobe, H.; Ando, W. *J. Am. Chem. Soc.* **1988**, *110*, 494 and references cited therein.

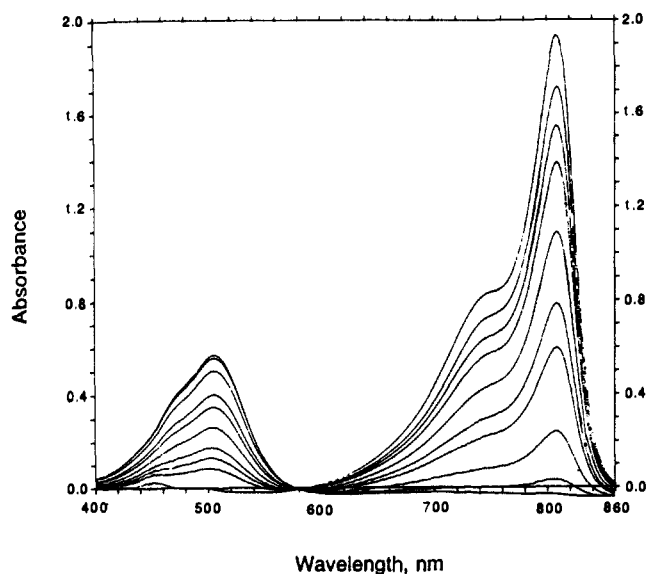


Figure 1. Isosbestic behavior for the conversion of **1j** (5×10^{-5} M) to **5d** in water. Total irradiation time was 3 min in a 1-cm-square quartz cell held 15 cm from a GE sunlamp. Sampling was every 5 s for the first three points, every 20 s for the next three, and every 35 s for the final three.

Table III. Absorption, Excitation, and Emission Spectral Data, Fluorescence Quantum Yields (Φ_{FM}), and Singlet Oxygen Quantum Yields [$\Phi(^1O_2)$] for Photooxidized Dyes **5**

compd	$\lambda_{max}(H_2O)$, nm	$\log \epsilon$	$\lambda_{EX}(H_2O)$, nm	$\lambda_{EM}(H_2O)$, nm	Φ_{FM}	$\Phi(^1O_2)^a$
5a	452	4.69	446	531	0.0031	
5b	480	4.72	464	551	0.0014	
5c	502	4.74	483	595	0.0008	≤ 0.004
5d	510	4.75	485	595	0.0004	

^a In air-saturated water (10% methanol).

the tellurapyrylium dyes yield products that absorb in the vicinity of 500 nm. The same products can be produced by self-sensitized dye photooxidation (vide infra) or by reaction with hydrogen peroxide (vide infra).

In water, the rate constant for reaction of **1j** with singlet oxygen was measured as $8 \times 10^8 \text{ M}^{-1} \text{ s}^{-1}$. This is 4.5-fold larger than the value in 50% aqueous methanol ($1.8 \times 10^7 \text{ M}^{-1} \text{ s}^{-1}$) and 100-fold larger than the value in 99% methanol ($9 \times 10^6 \text{ M}^{-1} \text{ s}^{-1}$). Under identical photooxidation conditions, the efficiency of methylene blue sensitized photooxidation of **1j** increases by a factor of 10 in deuterium oxide relative to water. This is consistent with the roughly 10-fold longer singlet oxygen lifetime in deuterated water.³⁰ The effect of deuteration on aqueous photooxidation efficiencies together with the similarities of the $k(^1O_2)$ values obtained with rose bengal and methylene blue support the involvement of singlet oxygen in the chalcogenapyrylium dye photobleach process.

Self-Sensitized Fade of Tellurapyrylium Dyes 1g-j. The reaction of tellurapyrylium dyes with singlet oxygen gives complete disappearance of the near-infrared absorption maximum. As shown in Figure 1, irradiation of an air-saturated, aqueous solution of **1j** (5×10^{-5} M) with an unfiltered tungsten bulb gave rapid disappearance of the dye chromophore and clean formation of a new product with an isosbestic point at 580 nm. Similar behavior was observed upon irradiation of aqueous solutions containing tellurapyrylium dyes **1h** and **1i** (isosbestic points at 550 and 560 nm, respectively). Dye **1g** gave a similar product but displayed poor isosbestic behavior. Spectral properties for the photooxidized materials are compiled in Table III. Self-sensitized photooxidation of dyes **1a-f** does not follow isosbestic behavior and gives colorless products. In carefully degassed aqueous solutions, no loss of

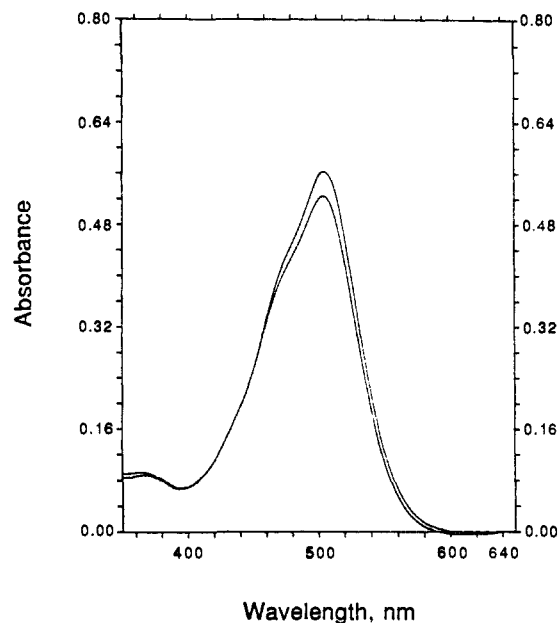
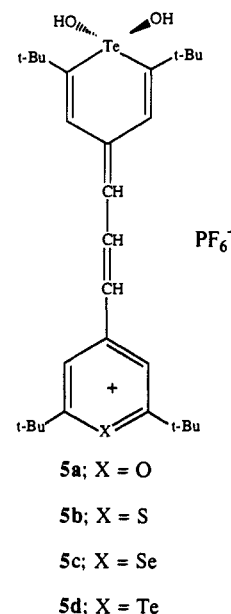


Figure 2. Comparison of the UV-visible absorption spectra of products produced by either the photooxidation of **1j** or the hydrogen peroxide oxidation of **1j**. Both products are identical and are identified as **5d**.

chromophore from tellurapyrylium dyes **1g-j** was observed after several hours of irradiation, suggesting that the presence of dioxygen was necessary for the photochemical reaction.

The reaction of a tellurapyrylium dye with singlet oxygen gives products that are derived from the formal oxidative addition of hydrogen peroxide across the tellurium atom to produce compounds of structure **5**. The addition of hydrogen peroxide to



aqueous solutions of **1g-i** generated the dyes **5**, identical spectroscopically (1H NMR, UV-vis) to the products of photooxidation (Figure 2). Rates of reaction between **1j** and hydrogen peroxide were measured both in 50% aqueous methanol and in water. A solution of 5×10^{-5} M **1j** and 0.01 M hydrogen peroxide was prepared in 50% aqueous methanol. The increase in absorption at 510 nm due to the formation of **5d** was monitored spectrophotometrically versus time in a 1-cm cell. A kinetic analysis yielded a pseudo-first-order rate constant of $3.3 \times 10^{-3} \text{ s}^{-1}$ at 23 °C corresponding to a second-order rate constant of $0.33 \text{ M}^{-1} \text{ s}^{-1}$. The rate constant is most accurately determined from the initial rate data since at longer times some loss of **5d** occurs. In water, **1j** was found to react more readily, necessitating the use of a concentration of hydrogen peroxide of 0.005 M for the

(30) (a) Merkel, P. B.; Kearns, D. R. *J. Am. Chem. Soc.* **1972**, *94*, 7244. (b) Rodgers, M. A. J. *J. Am. Chem. Soc.* **1983**, *105*, 6201.

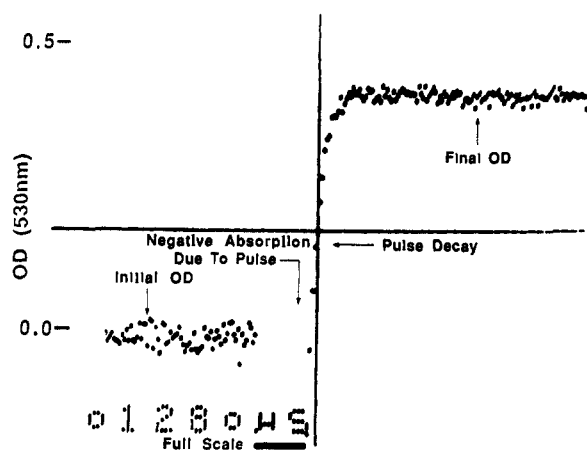


Figure 3. Time-resolved absorption at 530 nm reflecting the production of **5d** following UV-filtered xenon pulse excitation of 10^{-5} M **1j** in air-saturated 50% aqueous methanol in a 25-cm cell. The time scale is 5 μ s per point. The 530-nm absorption (representing about 4% conversion to product) is fully present or nearly so at the end of the exciting pulse, which decays over a period of approximately 50 μ s.

kinetics measurements. A second-order rate constant of $2.0 \text{ M}^{-1} \text{ s}^{-1}$ at 23 $^{\circ}\text{C}$ was determined in water, about six times as large as the value in 50% aqueous methanol. The rate constant for reaction of dye **1j** and hydrogen peroxide in deuterium oxide was found to be $1.8 \text{ M}^{-1} \text{ s}^{-1}$ at 23 $^{\circ}\text{C}$, which is identical with the water value within experimental uncertainty ($\pm 10\%$).

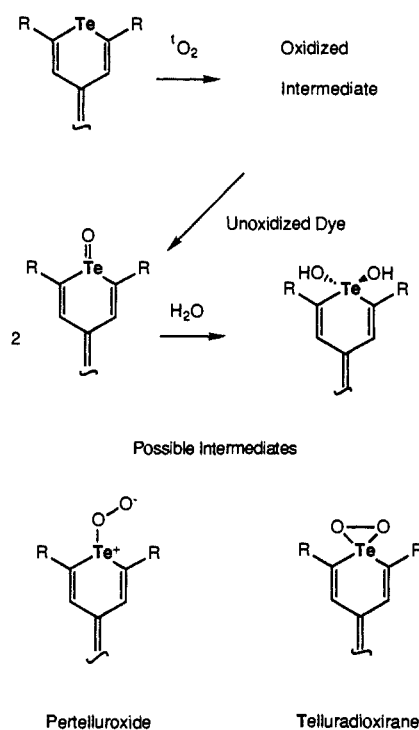
Flash Photolysis Studies. In view of the short lifetime of singlet oxygen, the self-sensitized bleaching of **1j** would be expected to occur within microseconds after absorption of a photon if a simple singlet-oxygen mechanism were operative. Since steady-state photolysis experiments indicate only that photooxidized products **5** are formed from **1g-j** within a few seconds, flash photolysis studies of the self-sensitized photooxidation of **1j** were carried out to provide some additional mechanistic insight. A 10^{-5} M solution of **1j** in air-saturated 50% aqueous methanol was excited in a 25-cm cell with a UV-filtered pulse from a xenon lamp. The pulse duration is roughly 100 μ s and the time required for 90% decay is about 50 μ s. The time-dependent increase in absorption at 530 nm, corresponding to formation of **5d**, was monitored with a beam from a xenon lamp, filtered through a monochromator, and detected with a photomultiplier tube and oscilloscope. The time-resolved absorption increase at 530 nm is shown in Figure 3, at a scale of 5 μ s per point.

From the absorption trace in Figure 3, it is evident that the formation of the 530-nm species is essentially complete by the time that the excitation pulse has decayed. No further increase in density is observed after approximately 50 μ s. Recalling the small rate constant ($0.3 \text{ M}^{-1} \text{ s}^{-1}$) for reaction between **1j** and hydrogen peroxide and noting that, if hydrogen peroxide were produced somehow photolytically, the concentration would not likely exceed the oxygen concentration of 2×10^{-3} M allows us to rule out hydrogen peroxide as the photooxidant. Thus, even though reaction with hydrogen peroxide yields the same product as photolysis, the rate of reaction with hydrogen peroxide is many orders of magnitude too low to account for the rapid photolytic formation of **5d**.

The rate of formation of **5d** is consistent with a singlet oxygen reaction. Since the lifetime of singlet oxygen in 50% aqueous methanol is about 6 μ s,³¹ the formation of **5d** directly by reaction with singlet oxygen would necessarily be complete in about 18 μ s (3 lifetimes).

The mechanism of oxidation of tellurapyrylium dyes by singlet oxygen can be compared to the well-studied oxidation of sulfides to sulfoxides.²⁹ The initial step for the oxidation of sulfides to sulfoxides is thought to be the formation of a persulfoxide or

Scheme I



thiadioxirane intermediate. This species then oxidizes an unoxidized sulfide molecule. Similar intermediates can be proposed for the reaction of the tellurapyrylium dyes with singlet oxygen followed by the initial oxidized intermediate reacting with unoxidized tellurapyrylium dye (Scheme I).

The oxidation of tellurapyrylium dyes **1g-j** with singlet oxygen does not give telluroxide products. Instead, the final products are hydrated forms of telluroxides. The hydration of telluroxides to give dialkyl and diaryl dihydroxy telluranes has been described³² and would be expected to be rapid in aqueous solvent.

If a reaction sequence such as Scheme I were proposed in which addition of singlet oxygen would be only the first step in the formation of **5**, then the subsequent steps would also be rapid. In this scheme, the reaction between **1j** and the initially formed oxidized intermediate (perhaps a pertelluroxide or telluradioxirane) would also have to be complete within about 50 μ s, based on the flash studies, at a concentration of **1j** at 10^{-5} M. Unless the lifetime of the oxidized intermediate is controlled by some other rapid decay process (such as the reverse reaction), the second-order rate constant for reaction between **1j** and the oxidized intermediate would have to be at least $2 \times 10^9 \text{ M}^{-1} \text{ s}^{-1}$, which is approaching the diffusion-controlled limit.

Values of $k(^1\text{O}_2)$ are quite sensitive to water concentration, increasing from $9 \times 10^6 \text{ M}^{-1} \text{ s}^{-1}$ in 99% methanol to $1.8 \times 10^8 \text{ M}^{-1} \text{ s}^{-1}$ in 50% aqueous methanol to $8 \times 10^8 \text{ M}^{-1} \text{ s}^{-1}$ in water. These values suggest that water is involved in the rate-determining step of the photooxidation. As shown in Scheme I, hydration might occur at either of two stages in the photooxidation: the addition of water to telluroxide intermediates is plausible or, alternatively, hydration of the initial oxidized intermediate might occur.

Some additional aspects of the flash photolysis experiment are worth noting. Although the concentration of **1j** is low in the flash experiment and the quantum yield for singlet oxygen production is about 0.12, the detection of the species absorbing at 530 nm is aided by the use of a 25-cm cell and by the possibility of multiple excitations of **1j**. Since the lifetime of the triplet state of **1j** is on the order of 0.3 μ s, a molecule of **1j** can conceivably be excited as many as 300 times during the course of the high-intensity 100- μ s pulse. This could produce a singlet oxygen concentration of up to 3×10^{-4} M. From the optical density increase at 530 nm and the extinction coefficient of **5d** ($56000 \text{ L mol}^{-1} \text{ cm}^{-1}$), a final

(31) The value of k_{dec} in 50% aqueous methanol was taken as the sum of $0.5k_{\text{dec}}$ in methanol ($1.0 \times 10^5 \text{ s}^{-1}$)^{30b} plus $0.5k_{\text{dec}}$ in water ($2.4 \times 10^5 \text{ s}^{-1}$),^{30b} which is equivalent to a lifetime of about 6 μ s.

(32) Detty, M. R. *J. Org. Chem.* **1980**, *45*, 274.

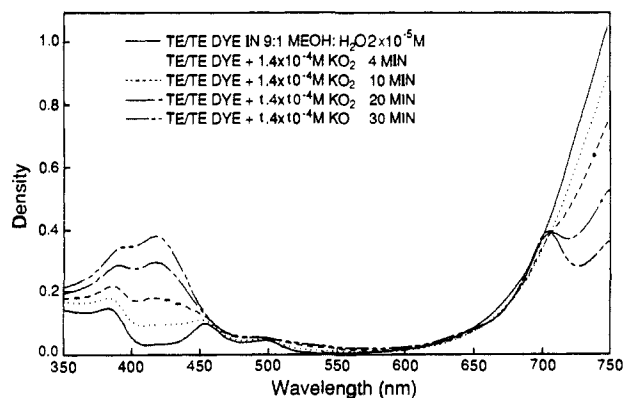


Figure 4. Spectral changes associated with the reaction of **1j** with superoxide radical anion.

Table IV. Excitation and Emission Data, Fluorescence Quantum Yields (Φ_{FM}), Calculated Radiative Lifetimes (τ_{rad}), Calculated Net Excited-State Lifetimes (τ_{net}), and Calculated Rate Constants for Intersystem Crossing (k_{isc}) for Chalcogenapyrylium Dyes **1** and **2d**

compd	$\lambda_{EX}(H_2O),^a$ nm	$\lambda_{EM},$ nm	Φ_{FM}	$\tau_{rad},$ ns	$\tau_{net},$ ns	k_{isc}, s^{-1}	E_{50}, cm^{-1}
1a	(552), 593	604	0.048	4.8	0.23	2×10^6	16 900
1c	(647), 686	698	0.011	7.3	0.08	8×10^6	14 600
1e	(650), 705						
1f	(652), 725	740	0.0024	8.1	0.02	7×10^8	13 700
1g	(650), 696	713	0.0050	10.1	0.05		14 300
1h	(653), 730	762	0.0014	12.0	0.02		13 200
1i	(655), 758	783	0.0004	15.0	0.006	2×10^{10}	13 000
1j	(660), 802	818	0.0004	13.2	0.005	4×10^{10}	12 300
2d	(646), 730	752	0.0003	11.1	0.003		13 200

^a Value in parentheses represents the excitation maximum of the H aggregate.

photoproduct concentration of 3×10^{-7} M is calculated. This represents a 3% conversion of **1j** to **5d** by a single pulse. If, in accordance with Scheme I, two molecules of **5d** are produced for every molecule of singlet oxygen that is scavenged, then only a 1.5×10^{-7} M concentration of singlet oxygen would need to be scavenged, or about 0.05% of the amount that could be produced by a single flash.

Reaction with Superoxide. Since it is possible that quenching of excited chalcogenapyrylium dyes by electron transfer to oxygen could lead to the formation of superoxide radical anion, reaction between **1j** and superoxide radical anion was investigated. To a methanol solution of 2×10^{-5} M **1j** containing 10% water was added 0.50 mg (1.4×10^{-4} M) of potassium superoxide (Aldrich). The resulting changes in visible absorption are shown in Figure 4. The reaction of **1j** with superoxide produces some **1g** (700-nm band) from tellurium–oxygen exchange and a second species that absorbs at approximately 420 nm. None of the photolytic product with absorption at 510 nm is detected by reaction with superoxide radical anion.

Emission Studies of Chalcogenapyrylium Dyes 1. The fluorescence emission spectra of many of the dyes **1** and **2d** have been measured (Table IV). The excitation and emission spectra are characterized by small Stokes shifts for the dyes **1** and **2d**, as shown in Figure 5 for the thiapyrylium dye **1c**. In the excitation spectra of the dyes **1**, the H-aggregate contribution is quite pronounced, as shown in Figure 5, and may be nearly as intense as the excitation maximum.

The quantum efficiencies of fluorescence, Φ_{FM} , are quite sensitive to the chalcogen atoms in the dye chromophore and vary in an inverse manner to the singlet oxygen yields. For example, Φ_{FM} decreases from 0.048 for **1a** to 0.0004 for **1j** while $\Phi(^1O_2)$ increases from 0.0004 for **1a** to 0.12 for **1j**. This behavior would be expected if variations in the rate of intersystem crossing from S_1 to T_1 were controlling both processes.

The estimated values for the net lifetime, τ_{net} , of the S_1 state and for the intersystem crossing rate constant, k_{isc} , in Table IV help to clarify the effects of heavy atoms on the photophysics of

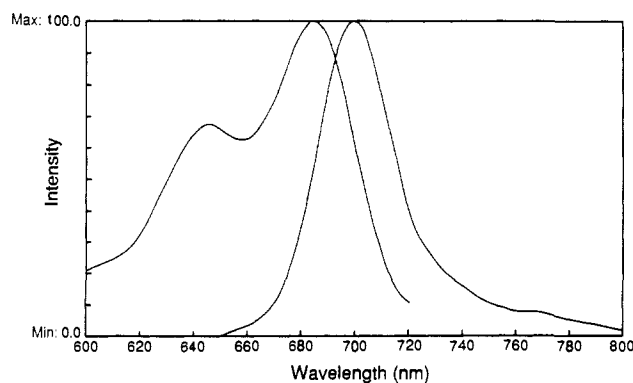


Figure 5. Excitation and emission spectra from **1c**. The excitation spectrum is characterized by strong excitation from the H-aggregate (short-wavelength excitation maximum). The emission spectrum is characterized by a small Stokes shift.

chalcogenapyrylium dyes. Attempts to measure τ_{net} experimentally for dyes **1e–h** were unsuccessful since lifetimes were shorter than 80 ps, the limit of resolution for our equipment. The radiative lifetime, τ_{rad} , can be approximated from the absorption spectra of the dyes while the product of τ_{rad} and Φ_{FM} yields an approximate τ_{net} .³³ As shown in Table IV, radiationless decay increases dramatically as the chalcogen atoms become heavier, with τ_{net} decreasing from approximately 230 ps for **1a** to about 5 ps for **1j**.

From the previously noted (vide supra) triplet yields and values of τ_{net} , the k_{isc} values in Table IV may be estimated.³³ It is evident that the heavy atom effect on k_{isc} is even more pronounced than the effect of τ_{net} . The former increases by four orders of magnitude for **1j** relative to **1a**. It is also evident from the values of k_{isc} and τ_{net} that the radiationless decay of the S_1 state is dominated by internal conversion rather than intersystem crossing. For example, the net decay constant for the S_1 state of **1j** (i.e., $1/\tau_{net}$) is approximately $2 \times 10^{11} s^{-1}$, which is an order of magnitude larger than k_{isc} . The contributions of k_{isc} to S_1 -decay decrease with decreasing chalcogen atomic weight, reducing to 0.05% for **1a**. Thus, while increases in S_1 internal conversion rates with increasing chalcogen weight tend to decrease triplet yields, this is more than offset by large increases in k_{isc} .

The introduction of methyl substituents to the methine backbones of monomethine dye **3** and trimethine dye **1f** to give **4** (from **3**) and **2d** and **2e** (from **1f**) decreases values of $\Phi(^1O_2)$. If this decrease were due to increased rates of internal conversion from increased steric interactions, then the changes in values of τ_{net} should parallel changes in $\Phi(^1O_2)$. The introduction of a methyl substituent in **1f** to give **2d** decreases the estimated τ_{net} by a factor of 6.7 (Table IV), which is somewhat greater than the 3.3-fold decrease in $\Phi(^1O_2)$.

Luminescence Studies Directed at Obtaining Triplet Energy Levels. The luminescence of dyes **1g** and **1j** was examined in alcohol solutions at room temperature, in glasses at 77 K, and in polymer films. The primary objective of these experiments was to locate triplet energy levels by obtaining phosphorescence spectra. The dyes **1g** and **1j** were excited with a high-intensity tungsten source through 700 and 750 nm narrow bandpass (10 nm) filters, respectively. Emission spectra were obtained, but luminescence signals associated with quantum efficiencies of less than roughly 0.0001 could not be distinguished from noise, even with cooling of the photomultiplier tube.

In methanol at ambient temperature, dye **1j** shows a weak luminescence that is a mirror image of the absorption spectrum and has an emission maximum at 840 nm. No significant emission was measured at wavelengths greater than 950 nm in either air-

(33) See ref 24. The radiative lifetime is approximated by the equation $\tau_{rad} = 3.5 \times 10^8 / (E_{50}^2 \epsilon_m \Delta\nu_{1/2})$, where E_{50} is the energy of the absorption maximum in cm^{-1} , ϵ_m is the molar extinction coefficient, and $\Delta\nu_{1/2}$ is the band width at half height in cm^{-1} . The net lifetime, τ_{net} , of the first excited state is then approximated by $\tau_{net} = \tau_{rad} \Phi_{FM}$, and the rate of intersystem crossing, k_{isc} , can be approximated by $k_{isc} = \Phi_T / \tau_{net}$, where Φ_T = triplet yield.

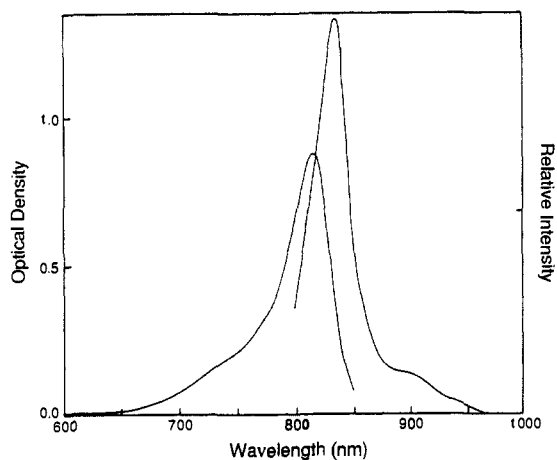


Figure 6. Absorption spectrum of 2×10^{-6} M **1j** in methanol and emission spectrum of **1j** in 4:1 ethanol:methanol glass at 77 K.

or nitrogen-saturated methanol. In a Butvar polymer film, emission intensity increases, but the spectrum is similar to that in methanol except for a shift of the emission maximum to 855 nm.

The luminescence of **1j** was also measured in a 4:1 ethanol:methanol glass at 77 K. Under these conditions, there is a substantial (about 5-fold) increase in fluorescence intensity relative to room temperature. The emission spectrum obtained is shown in Figure 6. The primary emission maximum is at 835 nm. There is a second band with an emission maximum at about 900 nm, which is similar to a shorter wavelength band in the absorption spectrum (Figure 6) and probably corresponds to vibronic structure. No resolvable luminescence was detected between 960 and 1100 nm.

With regard to phosphorescence from **1j**, three possibilities exist. Phosphorescence may be buried under the more intense fluorescence, possibly contributing to the absorption in the region of 900 nm. Phosphorescence may occur at a wavelength greater than 1100 nm. Finally, phosphorescence may have a quantum yield of less than 0.0001. Considering that the triplet quantum yield is 0.18, this would require a radiative rate constant of less than 0.0005 times the net decay rate, which is not unreasonable.

The luminescence from **1g** is more intense. In methanol at ambient temperature, the emission maximum is at 723 nm and mirrors the absorption spectrum. No additional luminescence is observed after deoxygenating the solution by nitrogen bubbling, suggesting that phosphorescence does not contribute significantly to the emission. The luminescence intensity of **1g** increases in polymer films or in ethanol-methanol glass at 77 K. As shown in Figure 7, the major emission band at 77 K has a maximum at 718 nm with a weaker band at about 770 nm and a shoulder at approximately 800 nm. At higher amplification, a very weak emission is apparent in the vicinity of 885 nm, which may be due to phosphorescence (or an additional vibronic fluorescence band).

If the weak emission at approximately 885 nm were due to phosphorescence from **1g**, the S_1-T_1 splitting in this molecule would be approximately 3000 cm^{-1} . This value is typical for the S_1-T_1 splittings found in other cationic dyes where a range of $1500-4500 \text{ cm}^{-1}$ has been found.²³ Data of Gilman indicate an S_1-T_1 splitting of 2900 cm^{-1} for 1,1'-diethyl-2,2'-cyanine.³⁴ An S_1-T_1 energy difference of 3000 cm^{-1} for **1j** would put T_1 at about 1070 nm (27 kcal/mol), above the energy required to generate singlet oxygen.

Some Properties of the Photooxidized Dyes 5. The in vivo photooxidation of tellurapyrylium dyes to products **5** would lead to a different class of materials whose properties might be of biological interest. The oxidized products absorb at much shorter wavelengths than their reduced counterparts **1** as shown in Table III. As a consequence, emission from the S_1 state of the oxidized dyes would be in the visible spectrum as shown in Figure 8 for

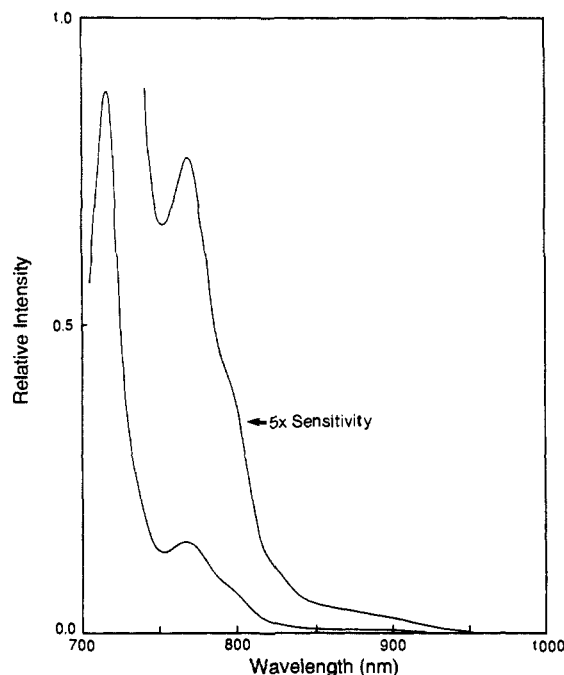


Figure 7. Emission spectrum of **1g** in 4:1 ethanol:methanol glass at 77 K.

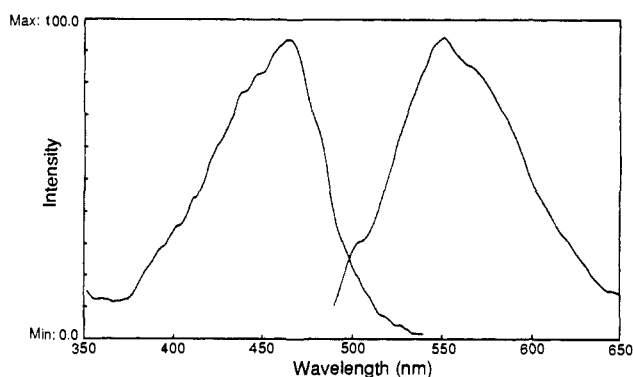


Figure 8. Excitation and emission spectrum of photooxidized product **5b**.

5b and compiled in Table III for the other oxidized dyes **5**. Quantum yields of fluorescence (Φ_{FM}) for these compounds are low and are similar to values obtained for reduced dyes **1g-j**. However, mitochondrial fluorescence has been observed by epifluorescence microscopy in cells where **5c** has been produced.^{19b}

The oxidized dyes **5** absorb around 500 nm and would presumably have triplet levels with sufficient energy to generate singlet oxygen. The use of a broad spectrum light source in PDT might excite the photooxidized dyes **5** in addition to the reduced dye **1**. As shown in Table III for dye **5c**, the quantum yield for singlet oxygen generation [$\Phi(^1O_2)$] is quite small and is at least 20-fold less than that of the reduced dye **1i**. (Some thermal loss of **5c** was observed.) The production of singlet oxygen upon in vivo irradiation of dyes **5** does not appear to be competitive with singlet oxygen produced by irradiation of dyes **1**.

Summary and Conclusions

Chalcogenapyrylium dyes of structure **1** appear to have potential as photosensitizers for use in photodynamic therapy. Selenapyrylium dyes and, in particular, tellurapyrylium dyes **1** have chromophores that extend well into the near infrared where biological tissues are most transparent. Heavy atom effects in seleno- and tellurapyrylium dyes allow reasonable quantum yields for triplet production and for singlet oxygen production. Binding of the dyes **1** to membranes both in vivo and in vitro may increase the yields of singlet oxygen. The in vivo production of singlet oxygen is a cytotoxic event for many cells. The heavy atom effects also lead to increased rates of radiationless decay from both the

(34) Gilman, P. B. *Photo. Sci. Eng.* 1967, 11, 222.

S_1 and T_1 states as the chalcogen atoms increase in mass. The net result is to shorten lifetimes of both the S_1 and T_1 states. Triplet yields increase from 0.0004 for **1a** to 0.18 for **1j** while quantum yields for singlet oxygen production increase from 0.0004 for **1a** to 0.12 for **1j**.

Tellurapyrylium dyes **1g-j** react much more rapidly than chalcogenapyrylium dyes **1a-f** with singlet oxygen to produce oxidized dyes **5**. Therapeutically, this property would be useful since deeper penetration of near-infrared light would be realized as the near-infrared-absorbing chromophore **1** reacts to give 500-nm-absorbing chromophore **5**. Singlet oxygen in combination with water produces the photooxidized materials **5**. The rate of reaction of hydrogen peroxide with **1g-j** is orders of magnitude too slow to account for the production of **5**, and the reaction of tellurapyrylium dyes with superoxide radical anion leads to products other than **5**.

In some instances, the lesser reactivity of the selenapyrylium dyes might be desirable for prolonged irradiation. Dyes **1e** and **1f** absorb at wavelengths of light above 700 nm. The incorporation of an additional heavy atom such as tellurium or iodine into the hydrocarbon backbone of **1e** and **1f** might lead to improved triplet yields and more efficient production of singlet oxygen.

Substitutions in the basic dye structure of **1** must be made judiciously to find improved sensitizers for PDT. Methyl substitution to give dyes **2** leads to increased radiationless decay in both the S_1 and T_1 states presumably via steric interactions. Decreases in both the quantum yields of fluorescence and the quantum yields of singlet oxygen production are observed in the dyes **2** and **4** when compared with the corresponding dyes **1** and **3**, respectively. The incorporation of additional heavy atoms into the hydrocarbon backbone should be made at positions where steric consequences would be minimal. Alternatively, rigidization of the dye molecules through the incorporation of the extended conjugation in rings might also increase the yields of singlet oxygen.

Experimental Section

Melting points were determined on a Thomas-Hoover melting point apparatus and are corrected. ^1H NMR spectra were recorded on a General Electric QE 300 instrument. Microanalyses were obtained with a Perkin-Elmer C, H, and N analyzer. Solvents (KODAK Laboratory Chemicals) were dried over 3A molecular sieves prior to use. UV-visible-near-IR spectra were recorded on a Perkin-Elmer Lambda 9 spectrophotometer. Emission quantum yields are compared to Rhodamine 6G as a standard ($\Phi_{\text{FM}} = 1.0$ in water), and relative quantum yields are corrected for changes in photomultiplier sensitivity as a function of wavelength.

General Procedure for the Preparation of Chalcogenapyrylium Dyes 1. A mixture of 1 mmol of 2,6-di-*tert*-butyl-4-methylchalcogenapyrylium hexafluorophosphate²² and 1.25 mmol of 2-(2,6-di-*tert*-butylchalcogenapyran-4-yl)acetaldehyde²² in 5 mL of acetic anhydride were heated in a 100 °C bath. Tellurapyrylium salts were heated for 5 min, selenapyrylium salts were heated for 10 min, and thiapyrylium and pyrylium salts were heated for 20 min. Following heating, the reaction mixtures were cooled to ambient temperature and were diluted with 5 mL of acetonitrile followed by 40 mL of ether. The resulting solutions were filtered through Celite and the filtrates were chilled, precipitating the dyes as crystalline solids. The solid materials were collected by filtration, washed with ether, and dried. The unsymmetrical chalcogenapyrylium dyes **1b**, **1d**, **1e**, and **1g-i** were recrystallized from 5 mL of acetonitrile and 25 mL of ether to give materials of greater than 98% purity by ^1H NMR. Compounds **1a** and **1b** were prepared as the perchlorate salts due to the availability of 2,6-di-*tert*-butyl-4-methylpyrylium perchlorate. While this particular perchlorate salt does not appear to be shock sensitive, care should be exercised when working with perchlorate salts due to their potential for being shock sensitive.

1a: 63%, mp 208–209 °C dec; λ_{max} (H_2O , log ϵ) 593 nm (5.31); ^1H NMR (CD_3CN) δ 8.55 (m, 1 H), 7.40 (br s, 2 H), 6.71 (br s, 2 H), 6.22 (d, 2 H, $J = 13.3$ Hz), 1.42 (s, 36 H). Anal. Calcd for $\text{C}_{29}\text{H}_{45}\text{O}_2\text{ClO}_4$: C, 66.59; H, 8.29. Found: C, 66.21; H, 8.36.

1b: 37%, mp 222.5–225 °C; λ_{max} (H_2O , log ϵ) 640 nm (5.32); ^1H NMR ($\text{MeOH}-d_4$) δ 8.44 (t, 1 H, $J = 13.3$ Hz), 6.42 (d, 1 H, $J = 13.3$ Hz), 6.17 (d, 1 H, $J = 13.3$ Hz), 1.45 (s, 18 H), 1.33 (s, 18 H). Anal. Calcd for $\text{C}_{29}\text{H}_{43}\text{OS-PF}_6$: C, 59.47; H, 7.40. Found: C, 59.42; H, 7.41.

1c: 65%, mp 198–201 °C; λ_{max} (H_2O , log ϵ) 685 nm (5.42); ^1H NMR (CD_3CN) δ 8.60 (t, 1 H, $J = 13.4$ Hz), 7.70 (br s, 4 H), 6.48 (d, 2 H,

$J = 13.4$ Hz), 1.47 (s, 36 H). Anal. Calcd for $\text{C}_{29}\text{H}_{43}\text{S}_2\text{PF}_6$: C, 57.88; H, 7.20; S, 10.66. Found: C, 57.58; H, 7.25; S, 10.83.

1d: 57%, mp 201–204 °C; λ_{max} (H_2O , log ϵ) 665 nm (5.38); ^1H NMR ($\text{MeOH}-d_4$) δ 8.41 (t, 1 H, $J = 12.5$ Hz), 6.52 (s, 1 H, $J = 12.5$ Hz), 6.30 (d, 1 H, $J = 12.5$ Hz), 8.0–6.3 (br, 4 H), 1.47 (s, 18 H), 1.39 (s, 18 H). Anal. Calcd for $\text{C}_{29}\text{H}_{43}\text{OSe-PF}_6$: C, 55.06; H, 6.85. Found: C, 54.96; H, 6.81.

1e: 73%, mp 222.5–225 °C; λ_{max} (H_2O , log ϵ) 708 nm (5.40); ^1H NMR (CD_3CN) δ 8.59 (t, 1 H, $J = 13.4$ Hz), 7.84 (br s, 2 H), 7.60 (br s, 2 H), 6.60 (d, 1 H, $J = 13.4$ Hz), 6.55 (d, 1 H, $J = 13.4$ Hz), 1.50 (s, 18 H), 1.47 (s, 18 H). Anal. Calcd for $\text{C}_{29}\text{H}_{43}\text{SSe-PF}_6$: C, 53.78; H, 6.65; S, 4.95. Found: C, 53.59; H, 6.39; S, 4.69.

1f: 76, mp 209–209.5 °C; λ_{max} (water) 730 nm (ϵ 300000); ^1H NMR (CD_3OD) δ 8.78 (t, 1 H, $J = 13$ Hz), 7.75 (br s, 4 H), 6.67 (d, 2 H, $J = 13$ Hz), 1.46 (s, 36 H). Anal. Calcd for $\text{C}_{29}\text{H}_{43}\text{Se}_2\text{PF}_6$: C, 50.15; H, 6.24. Found: C, 49.83; H, 6.06.

1g: 44%, mp 195–198 °C; λ_{max} (H_2O , log ϵ) 700 nm (5.27); ^1H NMR ($\text{MeOH}-d_4$) δ 8.29 (t, 1 H, $J = 12.5$ Hz), 7.8 (br s, 2 H), 7.2 (br s, 2 H), 6.70 (d, 1 H, $J = 12.5$ Hz), 6.45 (d, 1 H, $J = 12.5$ Hz), 1.45 (s, 18 H), 1.38 (s, 18 H). Anal. Calcd for $\text{C}_{29}\text{H}_{43}\text{OTe-PF}_6$: C, 51.21; H, 6.37. Found: C, 51.56; H, 6.49.

1h: 81%, mp 200.5–203.5 °C; λ_{max} (water) 745 nm (ϵ 110000); ^1H NMR (CD_3OD) δ 8.77 (t, 1 H, $J = 13$ Hz), 7.93 (br s, 2 H), 7.7 (br s, 2 H), 6.69 (d, 2 H, $J = 13$ Hz), 1.48 (s, 18 H), 1.42 (s, 18 H). Anal. Calcd for $\text{C}_{29}\text{H}_{43}\text{STe-PF}_6$: C, 50.03; H, 6.22; S, 4.60. Found: C, 50.08; H, 6.37; S, 4.99.

1i: 82%, mp 218–219 °C; λ_{max} (CH_2Cl_2) 786 nm (ϵ 304000); ^1H NMR (CD_3OD) δ 8.87 (t, 1 H, $J = 13.3$ Hz), 7.78 (br s, 4 H), 6.76 (d, 1 H, $J = 13.3$ Hz), 6.71 (d, 1 H, $J = 13.3$ Hz), 1.47 (s, 27 H), 1.45 (s, 9 H). Anal. Calcd for $\text{C}_{29}\text{H}_{43}\text{SeTe-PF}_6$: C, 46.87; H, 5.83. Found: C, 46.83; H, 5.74.

1j: 88%, mp 218–220 °C; λ_{max} (H_2O , log ϵ) 810 nm (5.18); ^1H NMR (CDCl_3) δ 8.75 (t, 1 H, $J = 13.5$ Hz), 7.71 (s, 4 H), 6.86 (d, 2 H, $J = 13.5$ Hz), 1.47 (s, 36 H). Anal. Calcd for $\text{C}_{29}\text{H}_{43}\text{Te}_2\text{PF}_6$: C, 43.99; H, 5.47. Found: C, 44.11; H, 5.34.

Preparation of 2a. 2,6-Di-*tert*-butyl-4-methyltellurapyrylium hexafluorophosphate (1.35 g, 2.9 mmol) and 2-(2,6-di-*tert*-butyltellurapyran-4-yl)propionaldehyde (1.0 g, 2.9 mmol) in 10 mL of acetic anhydride were heated at 100 °C for 10 min. The reaction mixture was diluted with 100 mL of ether, and the resulting mixture was filtered through Celite. The filtrate was chilled, precipitating the dye. The dye was collected by filtration and recrystallized from 3:1 ether-acetonitrile to give 0.80 g (34%) of **2a**: mp 182–185 °C; ^1H NMR (CD_2Cl_2) δ 8.55 (d, 1 H, $J = 13.5$ Hz), 7.93 (s, 2 H), 7.57 (s, 2 H), 6.75 (d, 1 H, $J = 13.5$ Hz), 2.31 (s, 3 H), 1.50 (s, 18 H), 1.48 (s, 18 H). Anal. Calcd for $\text{C}_{30}\text{H}_{45}\text{Te}_2\text{PF}_6$: C, 44.71; H, 5.63; Te, 34.1. Found: C, 44.47; H, 5.75; Te, 33.1.

Preparation of 2b. 2-(2,6-Di-*tert*-butyltellurapyran-4-yl)propionaldehyde (1.55 g, 4.40 mmol) and 2,6-di-*tert*-butyl-4-methylselenapyrylium perchlorate (1.30 g, 3.5 mmol) in 10 mL of acetic anhydride were heated at 100 °C for 20 min. The reaction mixture was diluted with 150 mL of ether and chilled. Large bronze crystals of **2b** were collected by filtration to give 1.01 g (41%) of material: mp 191–195 °C; ^1H NMR (CD_2Cl_2) δ 8.63 (d, 1 H, $J = 13.5$ Hz), 7.94 (s, 2 H), 7.57 (s, 2 H), 6.75 (d, 1 H, $J = 13.4$ Hz), 2.29 (s, 3 H), 1.50 (s, 18 H), 1.48 (s, 18 H). Anal. Calcd for $\text{C}_{30}\text{H}_{45}\text{SeTe-PF}_6$: C, 47.52; H, 5.98; Te, 16.8. Found: C, 47.92; H, 6.04; Te, 16.2.

Preparation of 2c. 2-(2,6-Di-*tert*-butyltellurapyran-4-yl)acetaldehyde (1.0 g, 3.0 mmol) and 4-ethyl-2,6-di-*tert*-butylselenapyrylium hexafluorophosphate (1.07 g, 2.5 mmol) in 10 mL of acetic anhydride were heated at 100 °C for 20 min. The reaction mixture was cooled to ambient temperature and diluted with 100 mL of ether. Chilling precipitated **2c** as bronze crystals that were collected by filtration to give 1.00 g of material: mp 198–199 °C; ^1H NMR (CD_2Cl_2) δ 8.63 (d, 1 H, $J = 13.5$ Hz), 7.94 (s, 2 H), 7.57 (s, 2 H), 6.75 (d, 1 H, $J = 13.4$ Hz), 2.29 (s, 3 H), 1.50 (s, 18 H), 1.48 (s, 18 H). Anal. Calcd for $\text{C}_{30}\text{H}_{45}\text{SeTe-PF}_6$: C, 47.52; H, 5.98; Te, 16.8. Found: C, 47.90; H, 6.14; Te, 16.3.

Preparation of 2d. 4-Ethyl-2,6-di-*tert*-butylselenapyrylium hexafluorophosphate²² (0.43 g, 1.0 mmol) and 2-(2,6-di-*tert*-butylselenapyran-4-yl)acetaldehyde³⁴ (0.33 g, 1.1 mmol) in 3 mL of acetic anhydride were heated at 100 °C for 10 min. The reaction mixture was diluted to 75 mL with ether and chilled. Bright green crystals of **2d** were collected by filtration to give 0.56 g (79%) of the dye: mp 182–185 °C; ^1H NMR (CD_3CN) δ 8.60 (d, 1 H, $J = 13.5$ Hz), 7.90 (s, 2 H), 7.64 (s, 2 H), 6.79 (d, 1 H, $J = 13.5$ Hz), 1.45 (s, 18 H), 1.41 (s, 18 H); λ_{max} (MeOH , log ϵ) 760 nm (5.38). Anal. Calcd for $\text{C}_{30}\text{H}_{45}\text{Se}_2\text{PF}_6$: C, 50.85; H, 6.40. Found: C, 50.81; H, 6.43.

Preparation of 2e. 4-Ethyl-2,6-di-*tert*-butylselenapyrylium hexafluorophosphate²² (4.29 g, 0.0100 mol) and 2-(2,6-di-*tert*-butyl-

selenapyranyl)propionaldehyde³⁴ (3.11 g, 0.0100 mol) in 10 mL of acetic anhydride were heated at 100 °C for 10 min. The reaction mixture was concentrated in vacuo. The residue was taken up in 5 mL of acetonitrile, filtered through glass wool, and diluted to 150 mL with ether. The resulting solution was chilled, precipitating the dye as purple-red plates (2.24 g, 31%): mp 165–168 °C; λ_{\max} (CH₂Cl₂, log ϵ) 782 nm (4.86); ¹H NMR (CD₃CN) δ 7.92 (br s, 1 H), 7.66 (s, 4 H), 2.22 (d, 6 H, J = 0.7 Hz), 1.44 (s, 36 H). Anal. Calcd for C₃₁H₄₇Se₂PF₆: C, 51.53; H, 6.56. Found: C, 51.35; H, 6.62.

Preparation of Dye 4. A mixture of 2,6-di-*tert*-butyltellurapyran-4-one (0.96 g, 3.0 mmol) and 2,6-di-*tert*-butyl-4-ethyltellurapyrylium hexafluorophosphate (1.41 g, 3.0 mmol) in 10 mL of acetic anhydride was heated at 100 °C for 10 min. The resulting solution was cooled to ambient temperature and was diluted with 100 mL of ether. The resulting solution was filtered through Celite and the filtrate was chilled. Long black needles of **4** precipitated and were collected by filtration. The needles were washed with ether and dried to give 0.58 g (25%) of **4**, mp 192–196 °C; ¹H NMR (CD₃CN) δ 7.61 (s, 4 H), 2.31 (s, 3 H), 1.37 (s, 36 H); λ_{\max} (MeOH) 772 nm (ϵ 41 000). Anal. Calcd for C₂₈H₄₃Te₂PF₆: C, 43.07; H, 5.55. Found: C, 43.21; H, 5.50.

Hydrogen Peroxide Oxidation of 1i and 1j. Hydrogen peroxide (100 μ L of a 30% solution, 1.0 mmol) was added via syringe to a solution of 1 mmol of **1i** or **1j** in 25 mL of methanol cooled to 0 °C. The resulting solution was stirred for 10 min at 0 °C and was then concentrated in vacuo. The maroon powder was washed with ether and collected by filtration to give **5c** and **5d** in 75% and 82% yields, respectively.

5d: ¹H NMR (MeOH-*d*₄) δ 8.88 (d \times d, 1 H, J = 12.0, 14.8 Hz), 8.68 (s, 2 H), 7.33 (s, 1 H), 7.28 (d, 1 H, J = 12.0 Hz), 6.72 (s, 1 H), 1.68 (s, 18 H), 1.52 (s, 9 H), 1.47 (s, 9 H); λ_{\max} (50% aqueous MeOH, log ϵ) 510 nm (4.75). Anal. Calcd for C₂₉H₄₃O₂Te₂PF₆: C, 42.95; H, 5.59. Found: C, 42.60; H, 5.61.

5c: ¹H NMR (MeOH-*d*₄) δ 8.81 (d \times d, 1 H, J = 12.0, 15.1 Hz), 8.69 (s, 2 H), 7.36 (s, 1 H), 7.33 (d, 1 H, J = 15.1 Hz), 7.07 (d, 1 H, J = 12.0 Hz), 6.74 (s, 1 H), 1.65 (s, 18 H), 1.52 (s, 9 H), 1.48 (s, 9 H); λ_{\max} (50% aqueous MeOH, log ϵ) 502 nm (4.74). Anal. Calcd for C₂₉H₄₃O₂SeTePF₆: C, 45.10; H, 5.87. Found: C, 45.23; H, 5.45.

Quantum Yields for Singlet Oxygen Generation in Methanol. Photolyses were carried out with light from a 500-W tungsten filament lamp filtered through appropriate narrow-band (10 nm) interference filters and cutoff filters. Irradiation intensity was monitored with an EG&G 450-1 radiometer calibrated vs a standard thermopile. Reinecke's salt actinometry³⁵ provided a calibration check. The singlet oxygen acceptor, 1,3-diphenylisobenzofuran (DPBF, purchased from Aldrich Chemical Co.), was recrystallized under yellow lights from an acetone–methanol mixture. Spectrograde methanol and certified rose bengal and methylene blue were used as received from Eastman Laboratory Chemicals.

Quantum yields for singlet oxygen generation in air-saturated methanol were determined by monitoring the chalcogenapyrylium-sensitized photooxidation of DPBF. DPBF is a convenient acceptor since it absorbs in a region of chalcogenapyrylium dye transparency and rapidly scavenges singlet oxygen to give colorless products. This reaction occurs with little or no physical quenching.³⁶ Our measurements of both rose bengal and methylene blue sensitized photooxidation of DPBF in methanol indicate that one molecule of this acceptor is destroyed per molecule of singlet oxygen scavenged. According to the procedure of Foote and co-workers,³⁷ the β -value for an acceptor and the quantum yield of singlet oxygen generation of a sensitizer may be determined from the slope and intercept of a plot of the inverse of the photooxidation quantum yield (Φ_{ox}) vs the inverse of the acceptor concentration. In this manner a β -value of 7.8×10^{-5} M was obtained for DPBF and a singlet oxygen quantum yield [$\Phi(^1\text{O}_2)$] of 0.77 ± 0.05 was obtained for rose bengal in methanol. The value of $\Phi(^1\text{O}_2)$ is very close to the literature value³⁸ of 0.76, which supports a one-to-one reaction between DPBF and singlet oxygen.

With use of a similar procedure with methylene blue as the sensitizer, a singlet oxygen quantum yield of 0.50 ± 0.05 and a β -value of 8.0×10^{-5} M were obtained. The $\Phi(^1\text{O}_2)$ value is reasonable on the basis of the reported³⁹ quantum yield for triplet formation of 0.52 in both ethanol and water and on the observation that oxygen quenching of methylene blue triplets in methanol produces singlet oxygen with nearly unit efficiency.^{30a}

Singlet oxygen quantum yields for the chalcogenapyrylium dyes were measured at low dye concentrations to minimize the possibility of singlet

oxygen quenching by the dyes. Irradiations were carried out in 2-cm cells containing a dye concentration (typically 2×10^{-6} M) sufficient to produce an optical density of approximately 0.3–0.5 at the irradiation wavelength. A DPBF concentration of 2×10^{-5} M was utilized.

The methylene blue sensitized bleach of DPBF (2×10^{-5} M) was measured with 2×10^{-6} M **1j** or **1i** added. The observed photobleaching quantum yields were the same with and without added dye within an experimental error of about 7%, indicating that rate constants for quenching of singlet oxygen (lifetime ≈ 10 μ s) by these dyes are $\leq 4 \times 10^9$ M⁻¹ s⁻¹ in methanol.

To simplify kinetic analysis, DPBF was photolyzed to low conversions ($\leq 10\%$) such that its concentration may be assumed to be fixed at the initial value. Photolyses required between 5 and 60 min, depending upon the efficiency of the chalcogenapyrylium photosensitizer. No thermal recovery of DPBF (from a possible decomposition of endoperoxide product) was observed under the conditions of these experiments. The quantum yield of singlet oxygen generation by a chalcogenapyrylium dye may be calculated by comparing the quantum yield for photooxidation of DPBF sensitized by the dye of interest to the quantum yield of methylene blue (MB) sensitized DPBF photooxidation at the same DPBF concentration:

$$\Phi(^1\text{O}_2)\{\text{dye}\} = [\Phi_{\text{ox,DPBF}}\{\text{dye}\}\Phi(^1\text{O}_2)\{\text{MB}\}] / \Phi_{\text{ox,DPBF}}\{\text{MB}\}$$

Alternatively, $\Phi(^1\text{O}_2)$ values for the chalcogenapyrylium dyes may be calculated from the following expression, using the measured β -value for DPBF:

$$\Phi(^1\text{O}_2)\{\text{dye}\} = \{\Phi_{\text{ox,DPBF}}\{\text{dye}\}(\beta + [\text{DPBF}])\} / [\text{DPBF}]$$

Values obtained by the two procedures were equivalent.

Rate Constants for the Reaction of Chalcogenapyrylium Dyes with Singlet Oxygen. Rate constants for reaction between the chalcogenapyrylium dyes and singlet oxygen were measured by photolyzing solutions containing a sensitizer with a known quantum yield for singlet oxygen generation [$\Phi(^1\text{O}_2)$] and a chalcogenapyrylium dye. The dye concentration was sufficiently low to have negligible effect on the decay of singlet oxygen. The quantum yield of sensitized chalcogenapyrylium dye photooxidation is given by

$$\Phi_{\text{ox,DYE}} = \Phi(^1\text{O}_2)k(^1\text{O}_2)\{\text{dye}\} / (k_{\text{dec}} + k(^1\text{O}_2)\{\text{dye}\}) \quad (5)$$

where $k(^1\text{O}_2)$ is the rate constant for photooxidation of chalcogenapyrylium dye, and k_{dec} is the rate constant for radiationless decay of singlet oxygen. At low concentrations of chalcogenapyrylium dye, this equation reduces to

$$\Phi_{\text{ox,DYE}} = \Phi(^1\text{O}_2)k(^1\text{O}_2)\{\text{dye}\} / k_{\text{dec}} \quad (6)$$

or

$$k(^1\text{O}_2) = \Phi_{\text{ox,DYE}}k_{\text{dec}} / \Phi(^1\text{O}_2)\{\text{dye}\} \quad (7)$$

A limited number of measurements were carried out in methanol with methylene blue as sensitizer. The $\Phi(^1\text{O}_2)$ value for methylene blue was taken as 0.50. The value of k_{dec} was taken as 1.0×10^5 s⁻¹.^{30b}

Rate constants for reaction with singlet oxygen for most of the chalcogenapyrylium dyes were measured in 50% (by volume) aqueous methanol with rose bengal as the sensitizer. Since very similar $\Phi(^1\text{O}_2)$ values have been measured for rose bengal in water (0.75)⁴⁰ and in methanol (0.76),³⁸ a value of 0.76 was utilized in 50% aqueous methanol. Rose bengal was excited at 544 nm, where light absorption by most of the chalcogenapyrylium dyes is quite low.

Values of $k(^1\text{O}_2)$ were also measured for several of the dyes with methylene blue as the sensitizer. Overlap of the chalcogenapyrylium dye and methylene blue absorption spectra precludes use of this combination for some of the chalcogenapyrylium dyes. For the methylene blue sensitizations, corrections were made for the chalcogenapyrylium dye absorption at the methylene blue excitation wavelength of 634 nm. The singlet oxygen yield obtained upon irradiation of methylene blue in air-saturated 50% aqueous methanol was taken as 0.50 on the basis of the triplet quantum yield of 0.52 in both ethanol and water,³⁹ on our measurements of $\Phi(^1\text{O}_2)$ of 0.50 ± 0.05 in both methanol and water, and on the aqueous value of 0.49 suggested by scavenging experiments with micellar DPBF.⁴¹

Solutions typically contained 6×10^{-6} M chalcogenapyrylium dye and either 6×10^{-6} M rose bengal or 8×10^{-6} M methylene blue. Most photolyses were carried out in a 1-cm cell for times ranging from 4 to

(35) Wegner, E. E.; Adamson, A. W. *J. Am. Chem. Soc.* **1966**, *88*, 394.

(36) Merkel, P. B.; Kearns, D. R. *J. Am. Chem. Soc.* **1975**, *97*, 462.

(37) Foote, C. S. In *Singlet Oxygen*; Academic: New York, 1979; p 139.

(38) Gollnick, K.; Schenck, G. O. *Pure Appl. Chem.* **1964**, *9*, 507.

(39) Nemoto, M.; Kokubun, H.; Koizumi, M. *Bull. Chem. Soc. Jpn.* **1969**, *42*, 1223, 2464.

(40) Gandin, E.; Lion, Y.; Van De Vorst, A. *Photochem. Photobiol.* **1983**, *37*, 271.

(41) Gorman, A. A.; Lovering, G.; Rodgers, M. A. J. *Photochem. Photobiol.* **1976**, *23*, 399.

60 min and at intensities spanning a 20-fold range depending upon chalcogenapyrylium dye reactivity. In some cases, lower chalcogenapyrylium dye concentrations were also used to check the validity of eq 6 for determining $k(^1\text{O}_2)$. Photooxidation rates were measured at conversion levels of $\leq 10\%$ to allow use of initial chalcogenapyrylium dye concentrations in eq 6. A k_{dec} value of $1.7 \times 10^5 \text{ s}^{-1}$ was used for 50% aqueous methanol.³¹

Methylene blue sensitized photooxidation efficiencies were also measured for **1j** in water and deuterium oxide. Solutions contained $3 \times 10^{-6} \text{ M}$ **1j** and $8 \times 10^{-6} \text{ M}$ methylene blue. A low dye concentration was used to minimize reduction of the relatively long singlet oxygen lifetime in deuterium oxide via reactive or physical quenching. A $k(^1\text{O}_2)$ value was calculated for **1j** in water with a k_{dec} of $2.4 \times 10^5 \text{ s}^{-1}$ and a value of $\Phi(^1\text{O}_2)$ for methylene blue of 0.50.^{30b}

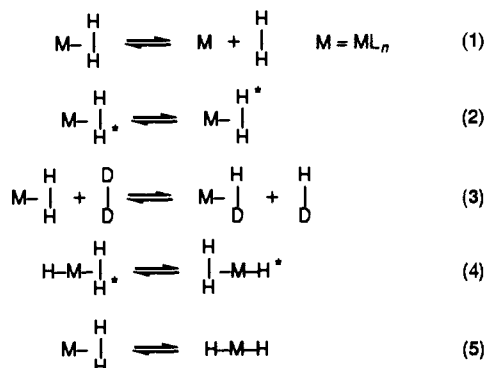
Molecular Hydrogen Complexes of the Transition Metals. 7. Kinetics and Thermodynamics of the Interconversion between Dihydride and Dihydrogen Forms of $\text{W}(\text{CO})_3(\text{PR}_3)_2\text{H}_2$ Where R = Isopropyl and Cyclopentyl

G. Rattan K. Khalsa,[†] Gregory J. Kubas,* Clifford J. Unkefer, Lori Stepan Van Der Sluys, and Kimberly A. Kubat-Martin

Contribution from Los Alamos National Laboratory, Inorganic and Structural Chemistry Group (INC-4), MS-C346, Los Alamos, New Mexico 87545. Received August 24, 1989

Abstract: Kinetic and thermodynamic parameters have been obtained for the equilibrium system $\text{H}_2\text{W}(\text{CO})_3(\text{PR}_3)_2 \rightleftharpoons \text{W}(\text{CO})_3(\text{PR}_3)_2(\eta^2\text{-H}_2)$. The systems studied include a newly synthesized complex where R = cyclopentyl. ³¹P NMR spin saturation transfer studies over a temperature range of 288–310 K afford values of $\Delta H^\ddagger = 10.1 \pm 1.8 \text{ kcal/mol}$, $\Delta S^\ddagger = -19.9 \pm 6.0 \text{ eu}$, and $\Delta G^\ddagger = 16.0 \pm 0.2 \text{ kcal/mol}$ (298 K) for the dihydrogen to dihydride exchange process where R = isopropyl. Exchange between nonequivalent hydrides in the seven-coordinate dihydride complex corresponds to $\Delta G^\ddagger \approx 11 \text{ kcal/mol}$ (253 K) derived from NMR coalescence data. ¹H^{[31}P] NMR equilibrium studies for the formation of the dihydrogen complex from the dihydride complex over the temperature range 265–309 K produce the following: $\Delta H^\circ = -1.2 \pm 0.6 \text{ kcal/mol}$, $\Delta S^\circ = -1.2 \pm 2.1 \text{ eu}$, and $\Delta G^\circ = -0.80 \pm 0.12 \text{ kcal/mol}$ (298 K) for R = isopropyl; $\Delta H^\circ = -1.5 \pm 0.4 \text{ kcal/mol}$, $\Delta S^\circ = -2.4 \pm 1.4 \text{ eu}$, and $\Delta G^\circ = -0.75 \pm 0.12 \text{ kcal/mol}$ (298 K) for R = cyclopentyl.

Although numerous $\eta^2\text{-H}_2$ -transition metal complexes have now been characterized,¹ no comprehensive thermochemical studies have been reported concerning the stability and energetics of dihydrogen coordination relative to classical hydride binding. Metal-bound dihydrogen/hydride systems exhibit a greater variety of dynamic behavior than any other ligand systems. The $\eta^2\text{-H}_2$ ligand undergoes reversible dissociation (eq 1), rotation about the M-H₂ axis (eq 2), isotopic scrambling (eq 3), exchange with hydride coligands (eq 4), and reversible cleavage to hydride ligands (oxidative addition, eq 5), all of which essentially can occur simultaneously and as equilibrium processes. In regard to eq 4,



activation parameters for intramolecular interchange of hydride and dihydrogen ligands have been measured for several cationic complexes.²⁻⁴ From a fundamental standpoint, eq 5 is the most significant of the above transformations because it represents not

only the key step in hydrogen activation but also *the breaking and re-forming of a metal-coordinated σ -bond as an equilibrium process*, a quite extraordinary situation. Such dynamic equilibria between dihydrogen and dihydride forms have been found to exist in solution for several complexes,⁵⁻⁹ including $\text{W}(\text{CO})_3(\text{PR}_3)_2\text{H}_2$,⁵ $[\text{CpRu}(\text{Me}_2\text{PC}_2\text{H}_4\text{PMe}_2)\text{H}_2]\text{BF}_4$,⁶ and $[(\text{C}_5\text{Me}_5)\text{Re}(\text{CO})(\text{NO})\text{H}_2]\text{BF}_4$,⁷ with the H₂ form being predominant (essentially 100% in the solid state). Terminology-wise, "isomerism" or "tautomerism" seems inadequate to describe the situation here, since relatively large changes in metal-ligand geometry, coordination number, and formal oxidation state are involved. The seven-coordinate dihydride "tautomer" of the tungsten complex is stereochemically nonrigid on the NMR time scale, adding yet a further dimension to the already rich dynamics of this system.⁵ The rate of oxidative addition of bound $\eta^2\text{-H}_2$ to produce the dihydride form of the Ru complex was reported to be considerably lower than that in the tungsten system (as estimated from pub-

(1) Kubas, G. J. *Acc. Chem. Res.* **1988**, *21*, 120. Kubas, G. J. *Comments Inorg. Chem.* **1988**, *7*, 17.

(2) Morris, R. H.; Sawyer, J. F.; Shiralion, M.; Zubkowski, J. D. *J. Am. Chem. Soc.* **1985**, *107*, 5581.

(3) Bautista, M. T.; Earl, K. A.; Morris, R. H.; Sella, A. *J. Am. Chem. Soc.* **1987**, *109*, 3780.

(4) Bautista, M. T.; Earl, K. A.; Morris, R. H. *Inorg. Chem.* **1988**, *27*, 1124.

(5) (a) Kubas, G. J.; Ryan, R. R.; Wroblewski, D. A. *J. Am. Chem. Soc.* **1986**, *108*, 1339. (b) Kubas, G. J.; Unkefer, C. J.; Swanson, B. I.; Fukushima, E. *J. Am. Chem. Soc.* **1986**, *108*, 7000.

(6) Chinn, M. S.; Heinekey, D. M. *J. Am. Chem. Soc.* **1987**, *109*, 5865. (7) Chinn, M. S.; Heinekey, D. M.; Payne, N. G.; Sofield, C. D. *Organometallics* **1989**, *8*, 1824.

(8) Bianchini, C.; Mealli, C.; Peruzzini, M.; Zanobini, F. *J. Am. Chem. Soc.* **1987**, *109*, 5548.

(9) (a) Arliguie, T.; Chaudret, B. *J. Chem. Soc., Chem. Commun.* **1989**, 155. (b) Mura, P.; Segre, A.; Sostero, S. *Inorg. Chem.* **1989**, *28*, 2853. (c) Cappellani, E. P.; Maltby, P. A.; Morris, R. H.; Schweitzer, C. T.; Steel, M. R. *Inorg. Chem.* **1989**, *28*, 4437.

[†] On leave of absence from the Department of Chemistry, Thiel College, Greenville, PA.